IAC-14,A3,P,42,x24325

USING RADIATION PRESSURE TO CONTROL ORBITS AROUND A TRIPLE ASTEROIDE

Thais Carneiro Oliveira
National Institute for Space Research (INPE), Brazil, thais.tata@gmail.com

Antonio Fernando Bertachini de Almeida Prado
National Institute for Space Research (INPE), Brazil, prado@dem.inpe.br

It is believed that most of the asteroids keep information about the original composition of the Solar System, so it is of great scientific interest to study those bodies. One of the most interesting candidates for a mission is the asteroid 2001 SN_{263}. It is a triple system, which components have radius about 1.30 km, 0.39 km and 0.29 km. Using a reference system centered in the larger body, the second component is in an orbit that has semi-major axis of 16.63 km and eccentricity 0.015, and the third component is in an orbit with semi-major axis of 3.80 km and eccentricity 0.016. Currently, there are several institutions in Brazil studying a mission to this asteroid. This mission is called ASTER and it is planned for an one year duration in the asteroid system. The goal of the present paper is to study the forces acting in that system, and then verify the possibility of using the solar radiation pressure to make station-keeping maneuvers. The dynamical model will consider the main forces acting on that system, including the gravitational forces of the three bodies of the system, the J_2 perturbation of the main body and the solar radiation pressure. For a given orbit, the optimal direction of the solar sail attitude along the orbit is found, as well as the size that the solar sail must have in order to compensate the disturbing forces. Optimal solutions will be searched by allowing variations of those parameters. Also, a sub-optimal analysis is considered by fixing the area of the solar sail but maintaining the optimal solar sail attitude. The necessity of a propulsion system to complement the maneuvers will be considered. A large number of orbits will be tested, around the three bodies of the system.

I. INTRODUCTION

Asteroids are defined as bodies that orbit the Sun but are too small to be considered a planet, according to the IAU definition[1]. The NEA ("Near Earth Asteroid") is an asteroid that has a trajectory that brings them within 1.3 AU from the Sun and hence within 0.3 AU of the Earth's orbit[2]. The triple system asteroid studied in this paper is a NEA and it is known as NEA 2001 SN_{263}.

The NEA 2001 SN_{263} is the target for the Brazilian mission called ASTER, which aims to have a spacecraft orbiting the main body of the asteroid system[3]. The mission towards this asteroid has a great advantage for the scientific studies since it is a NEA triple system asteroid.

This paper is concerned with the evaluation of the magnitude of the main perturbations that act on a spacecraft orbiting the main body of this asteroid and, moreover, the potential use of a solar sail to reduce the deviations caused by these perturbations for an orbiting spacecraft.

There are two main reasons to study the asteroids and to consider missions forwarded them. One is to increase the knowledge of the formation and the composition of the solar system by studying asteroids[4,5]. The asteroids maintain some vital information about the origins of the solar system, weather by their dynamical motion or by their chemical composition and internal structure. In this way, asteroids can help the scientific community to understand more about the beginning and the evolution of the solar system[4].

In addition, the NEA asteroids could be a catastrophic threat to life on Earth if one of then collide with the surface of the Earth. Therefore, the knowledge of the composition and dynamics of these bodies is essential to help humanity to prevent a possible catastrophe as well as to understating the dynamics and composition of these threats[4,5].

The perturbations that act on the spacecraft orbiting the larger body of the asteroid system considered in this paper are: the solar radiation pressure, the third-body gravitational perturbation of the two smaller bodies that belongs to the asteroid system and of the Sun, and the J_2 perturbation of the main body.

The triple system 2001 SN_{263}

The asteroid 2001 SN_{263} was discovered in 2001 by the LINEAR ("Lincoln Near-Earth Asteroid Research") program[4].

The discovery that the asteroid was really a triple system occurred in 2008, when a radio-astronomy station of Arecibo, in Puerto Rico, analysed this asteroid for 16 days[4,6].

The currently knowledge of the physical aspects of this asteroid, as well as the dynamical motion and other important parameters, are given in Table 1:[4,7,8]

Body	Orbits	a^8	e^8	I^8	Mass[8]
Alpha (α)	Sun	1.99 au	0.48	6.7°	917.47 x 10^{10} kg
Beta (β)	Alpha	16.63 km	0.015	0.0°	24.04 x 10^{10} kg
Gamma (γ)	Alpha	3.80 km	0.016	$\approx 14°$	9.77 x 10^{10} kg

Table 1: Physical parameters of the system 2001 SN$_{263}$

where "a" is the semi-major axis, "e" is the eccentricity and "I" is the inclination of Alpha related to the ecliptic plane and the inclination of Beta and Gamma are measured with respect to the equator of Alpha.

The J_2 constant for the oblateness of the central body Alpha considered in this work is $J_2 = 0.013$ and its radius is $R_e = 1.3$ km[8].

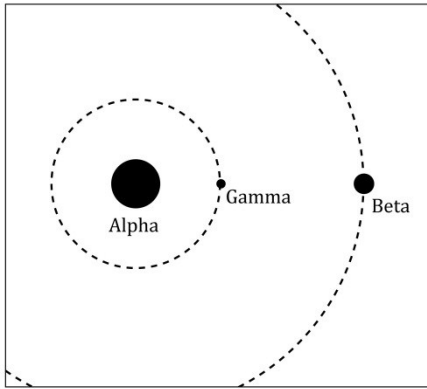Figure 1 illustrates the triple system 2001 SN$_{263}$.

Fig. 1: Representation of the triple system 2001 SN$_{263}$.

II. THE MATHEMATICAL MODEL

This section contains the mathematical models used in this paper, which includes the perturbation formulation, the solar sail design and considerations and the method for the evaluation of the magnitude of the perturbations, named perturbation integral.

The Perturbation Integral

The perturbation integral ("PI") is actually the integral for one orbital period of the normalized acceleration of the disturbing forces that act on the spacecraft. The equation for the PI is given by: [9,10,11,12,13]

$$PI = \int_0^T |\mathbf{A}|\, dt \qquad [1]$$

where $\mathbf{A}$ is the acceleration vector of the disturbing forces, t is the time and T is the period of the orbit of the spacecraft.

In addition, it is also important to consider the trajectory and the motion of the third-bodies in Equation 1. The motion of the bodies Alpha, Beta and Gamma

can be considered by solving the Kepler's equation for every step of the time.

The PI is actually the amount of velocity variation that the external perturbations deliver to the spacecraft for one orbital period. The norm of the acceleration means that the spacecraft remains in a Keplerian orbit all the time. In this way, the PI is the fuel consumption if it is assumed that a propulsion system corrects the shifts caused by the external forces all the time, by applying a force with the same magnitude but opposite direction of the disturbing forces. [9,10]

The PI integral measure the total effects of the magnitude of the disturbing forces that act on the spacecraft. It is possible to create maps with the PI values versus the variation of the Keplerian elements of the orbit. The maps can be very useful to plan a mission by analysing the orbits that are less perturbed and to know the magnitude of the perturbation for a given orbit.

In this paper, the perturbation integral is also used to evaluate the amount of the magnitude perturbation reduction that the solar sail can accomplish[14].

The Averaging Technique for the Perturbation Integral

The PI, as formulated in Equation (1), provides the amount of velocity change that the spacecraft receives from the disturbing forces for a specific configuration. In order to have a result that is more general and that presents the mean value of the PI for all possible configurations, an averaging technique is used in this work. The averaging technique consists in integrating the PI for different initial positions of the third bodies or the main body. The averaging technique is formulated as follows[9]:

$$KPI = \frac{1}{2\pi}\int_0^{2\pi} PI\, dE_0 \qquad [2]$$

where E_0 is the eccentric anomaly of the third-body or of the main body. The KPI is the PI after applying the averaging technique explained above. Equation (2) is valid only for the analysis of a single disturbing force. The J_2 perturbation does not need the averaging technique in this work, since it was considered that Alpha does not rotate around a fixed axis and so it remains steady.

If more than one disturbing force is considered, it may be necessary to perform an average over the positions of the three bodies, so the KPI becomes[9,11]:

$$KPI = \frac{1}{(2\pi)^3}\iiint_0^{2\pi} PI\, dE_\alpha\, dE_\beta dE_\gamma \qquad [3]$$

The averaging technique in Equation 3 includes all the possible initial configurations this system can have.

The Third-Body Perturbation

The third-body perturbation is caused by the gravitational attraction of a third body that does not include the main central body and the spacecraft. This gravitational attraction of the third body leads to a disturbance on the spacecraft trajectory, deviating it from a Keplerian orbit.

In this work, for the system NEA 2001 SN_{263}, the third-body perturbations considered are caused by Gamma, Beta and the Sun.

The equation that describes the acceleration of the third-body (A_{tb}) is given by[9,12,15]:

$$A_{tb} = Gm_0 \left(\frac{r_{s0}}{r_{s0}^3} - \frac{r_{\alpha 0}}{r_{\alpha 0}^3} \right) \qquad [4]$$

where m_0 is the mass of the third-body, r_{s0} is the position vector that starts at the spacecraft and that ends in the center of mass of the third-body, $r_{\alpha 0}$ is the position vector that starts at the center of mass of the main body (Alpha) and that ends in the center of the third-body and G is the universal gravitational constant.

The value considered for the universal gravitational constant is G = 6.67259x10^{-11} m³/kg/s². The mass of the Sun is considered to be m_{Sun}= 1.9889 x 10^{30} kg and 1 au is equivalent to 1.49597871x10^{8} km [9,10,11]. Figure 2 illustrates the third-body perturbation formulated by Equation 2[15].
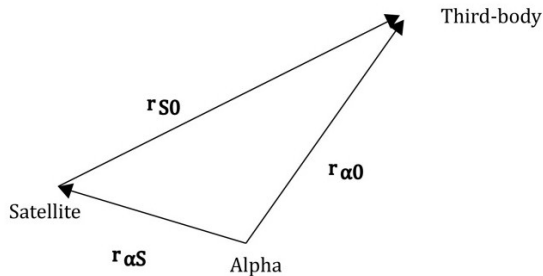

Fig. 2: Illustration of the third-body perturbation formulation.

The Oblateness of the Main Body Alpha

The main body of the triple system 2001 SN_{263}, Alpha, is not perfectly spherical. The most prominent perturbation derived from this non-spherical body is due to its oblateness. This irregularity of the body can be mathematically formulated with the help of the J_2 coefficient[15].

The J_2 coefficient, therefore, is a measure of the oblateness of the body and, for Alpha, its value is J_2 = 0.013[8].

The acceleration perturbation due to the gravity of the oblateness Alpha (A_{J2}) is given as follows[15]:

$$A_{J2} = \frac{3Gm_\alpha J_2}{r_{\alpha S}^2} \left(\frac{R_e}{r_{\alpha S}} \right)^2 \begin{bmatrix} P_2(cos\emptyset)\hat{g}_r + \\ cos\emptyset sin\emptyset \ \hat{g}_\emptyset \end{bmatrix} \qquad [5]$$

where m_α is the mass of the body Alpha, $r_{\alpha S}$ is the distance from the spacecraft to Alpha, R_e is the equatorial radius of Alpha ($R_e = 1.3 \ km$)[8], P_2 is the Legendre polynomial of second degree, $\hat{g}_r$ is the radial unit vector direction and $\hat{g}_\emptyset$ is the southward unit vector direction and both of these unit vectors are in the local horizon frame.

The Solar Radiation Pressure

The solar radiation pressure is another disturbing force considered that deviates the spacecraft from the Keplerian orbit.

The solar radiation pressure is actually the change of momentum from a light beam coming from Sun and colliding with the surface of the spacecraft. This change of energy results in a force acting on the surface of the spacecraft.

This force can result in a torque if the resulting force is not directed to the center of mass of the spacecraft. If there is a resulting force directed to the center of mass, the spacecraft can be deviate from its nominal orbit[16,17].

This paper will only consider the solar pressure force acting on the centre of mass of the spacecraft. It is assumed that the spacecraft has a smooth rectangular shape and that one of its faces is always pointed towards the Alpha body. Each face of the rectangular side of the spacecraft has 50 m², the mass of the spacecraft is 200 kg and the reflectivity coefficient ε is 0.8. The reflectivity coefficient multiplied by 100 is actually the percentage of light flux that is reflected by the material of the surface. For this spacecraft, 80% of the light flux is reflected by the surface and 20% of it is absorbed by the surface.

The mathematical formulation for the acceleration of the solar radiation pressure for a smooth surface is given as follows[16].

$$A_{sr} = \frac{h(1+\varepsilon)}{c} \left(\frac{R}{r_S} \right)^2 \frac{S}{m} cos^2\delta \ \hat{f} \qquad [6]$$

where h is the power of the solar radiation per area (h = 1.35x10[6][erg/cm² - sec] for the region around the Earth), c is velocity of the light, r_S is the distance from the spacecraft to the Sun, R is the distance from the Earth to the Sun, S is the area of the spacecraft that is illuminated, m is the mass of the spacecraft, δ is the incidence angle that the opposite direction of the light flux makes with the normal and the illuminated surface and $\hat{f}$ is the unit vector that indicates the direction of the solar radiation force. The multiplication by $\left(\frac{R}{r_S} \right)^2$ allows

the use of Equation (3) for any distance of the spacecraft to the Sun. The Figure 3 illustrates the light interaction with the surface[16].
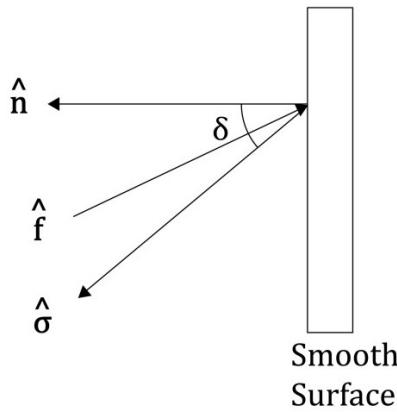

Fig. 3: The solar radiation interaction with a smooth surface.

where $\hat{\boldsymbol{\sigma}}$ is the opposite direction of the incidence of the solar ray, δ is the incidence angle of light, $\hat{\boldsymbol{n}}$ is the direction of the normal of the surface and $\hat{\boldsymbol{f}}$ is the direction of the force of the solar sail radiation.

The unit vector $\hat{\boldsymbol{f}}$ is given by Equation 7[16]:

$$\hat{\boldsymbol{f}} = -\frac{(1-\varepsilon)\hat{\boldsymbol{\sigma}} + 2\varepsilon cos\delta\hat{\boldsymbol{n}}}{\sqrt{(1-\varepsilon)^2 + 4\varepsilon cos^2\delta}} \qquad [7]$$

Another important consideration is the shadow created by the geometry of Alpha and the Sun. There may be some shadow on the path of the spacecraft and when it occurs, the solar sail radiation can be reduced or even zeroed. The shadow considered in this work is based on the geometry of the Sun, Alpha and the spacecraft, obtained by conical projections. There are three possible solutions for these projections: illumination, penumbra or umbra. The penumbra region is actually a region that has only half of the energy of the solar radiation; therefore, Equation 6 is multiplied by ½ if the spacecraft is in this area. If the spacecraft is on the umbra region, then the solar radiation pressure is zeroed [18].

The Solar Sail

The main focus of this work is to use the solar sail to reduce or eliminate the external perturbations that act on the spacecraft by applying a force in the opposite direction. In order to use the solar radiation pressure as a propulsion system that reduces the other perturbation forces, the direction of the force caused by the solar sail $\hat{\boldsymbol{f}}_{ss}$ must be opposite to the sum of all perturbations[13].

The solar sail is considered to have a smooth area also, but its area can be either fixed or variable. The variable area for the solar sail permits the control of the magnitude of the solar sail perturbation, therefore if there is light and the incidence angle is lower than 90 degrees, the solar sail can eliminated completely the others perturbations. If the solar sail has a fixed area, the magnitude of the perturbation cannot be controlled, although the solar sail can still reduce the other perturbation forces[13].

The attitude of the solar sail is actually defined by the unit vector direction $\hat{\boldsymbol{f}}_{ss}$ of the solar sail. The solar sail reflectivity coefficient considered in this work is ε=1. Therefore, $\hat{\boldsymbol{f}}_{ss} = -\hat{\boldsymbol{n}}$ (see Equation 7 and Figure 3). The incidence angle δ can be found by the expression $cos\delta = \hat{\boldsymbol{n}} \cdot \hat{\boldsymbol{\sigma}}$.

If there is a shadow on the solar sail, it is not possible to use it to reduce the perturbations. Also if the incidence angle δ necessary to reduce the perturbations is larger than 90 degrees, the solar sail cannot reduce or eliminate the other perturbations. In the case of an incidence angle larger than 90 degrees, the solar sail becomes inactive. To inactivate the solar sail, one solution is to build it with a thin base area, so when the solar sail has this thin base faced the Sun, its perturbation can be disregarded[13].

It is important to point out also that it is assumed that the solar sail can rotate freely to have an optimal attitude to reduce the other perturbations.

III. RESULTS

This section presents the results based on the theory mentioned in the mathematical model. The first sub-section of the results contains maps of the KPI integrals for different orbits and different disturbing forces.

The second sub-section presents the usage of a solar sail for a specific configuration and a certain number of orbits to analyse the reduction of the disturbing forces.

Mapping the Asteroid 2001 SN$_{263}$ with KPI values

Figures 4 and 5 present the KPI value for different disturbing forces as the semi-major axis changes. The orbits are circular and equatorial ($e = 0$ and $I = 0°$).

As the semi-major axis increases, the period of the orbit also increases, leading to an increase of the KPI values. In order to have time independent KPI values, all of the KPI values were multiplied by a nominal orbital period of a circular equatorial orbit with 9300 km of semi-major axis and divided by the current orbital period.
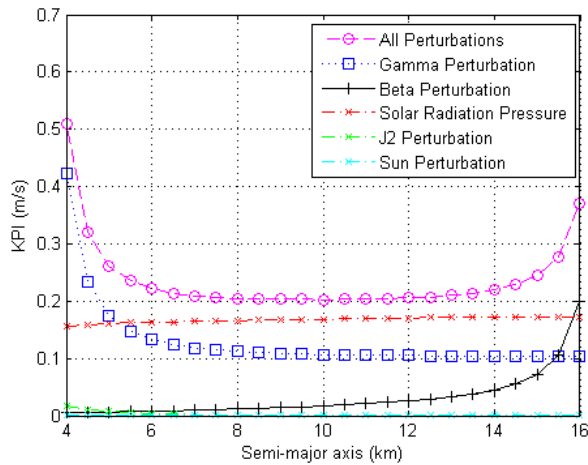
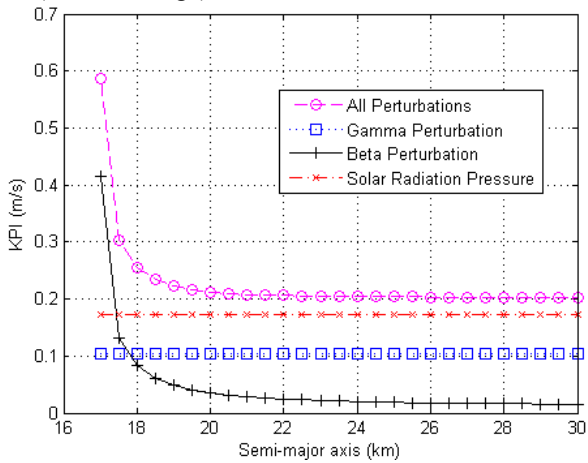Fig. 4: The KPI values as the semi-major axis increases (4-16 km range).

Fig. 5: The KPI values as the semi-major axis increases (17-30 km range).

As shown in Figure 4, the J$_2$ and the Sun perturbations have a low value if compare to the other perturbations. Actually, the J$_2$ perturbation is larger than the Beta perturbation until the semi-major axis of 5.1 km. For larger values of this semi-major axis, the Beta perturbation is larger than the J$_2$ perturbation. As described by Equation 5, the J$_2$ perturbation decays exponentially as the distance from the main body increases. The J$_2$ perturbation has a KPI = 0.018 m/s at 4 km of semi-major axis and KPI = 7x10^{-3} m/s at 5.1 km semi-major axis.

The solar radiation pressure perturbation acting on the spacecraft increases smoothly when the semi-major axis increases. For low values of the semi-major axis, the spacecraft has the chance to be in the shadow of the Alpha body and it helps to decrease the magnitude of solar radiation pressure. Also, the energy emitted by the Sun is inversely proportional to its square distance, so the solar radiation pressure increases slowly as the semi-major axis increases and the distance from the Sun decreases.

Concerning the third-body perturbation of the Gamma and Beta bodies, it is clear that the third-body perturbation increases as the spacecraft semi-major axis approaches the third-body semi-major axis and it decreases exponentially and as the spacecraft departs from the body (see Equation 4).

The solar radiation pressure is the most eminent perturbation for the range of semi-major axis considered. Nevertheless, the sum of all perturbations is not the sum of each individual perturbation, since the sum of the perturbations occurs before considering the norm of the acceleration (see Equation 1).

It is important to note that the Gamma perturbation tends to KPI = 0.103 m/s and the Beta tends to KPI = 0.015 m/s as the semi-major axis increases. These perturbations tend to a certain value different from zero because of the second part of the right-hand side in Equation 4, where the perturbation is related to the distance from the third-body and the main body. It means the indirect term of the perturbation acts to perturb the orbit of the spacecraft, even when its orbit is very large.

There is a minimum in Figure 4 for the KPI value regarding the sum of all perturbations and it occurs at the semi-major axis equal to 9.32 km. The KPI value at Figure 4 is almost steady for a large range of the semi-major axis and the minimum value of it at a = 9.32 km is practically the same for a > 25 km. In this way, if the orbit of the spacecraft must be between Gamma and Beta, the best semi-major axis would be a = 9.3 km but some small deviations of this value of the semi-major axis will not increase significantly the disturbances that the spacecraft receives. If there is a necessity to have a spacecraft after the orbits of Gamma and Beta, then it is best to consider orbits with a >20 km, so the change of the disturbing forces will be again smoothly and minor.

Figures 6 and 7 show the variation of the KPI value for different values of the eccentricity. The semi-major axis of the orbit was chosen to be 9.3 km (the minimum KPI value for the semi-major axis), and the inclination is equal to zero.
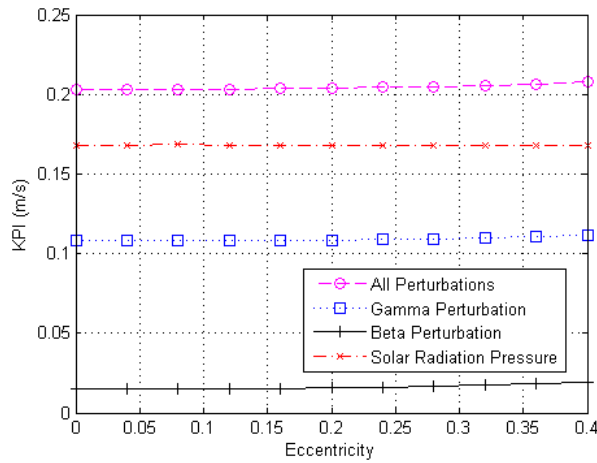
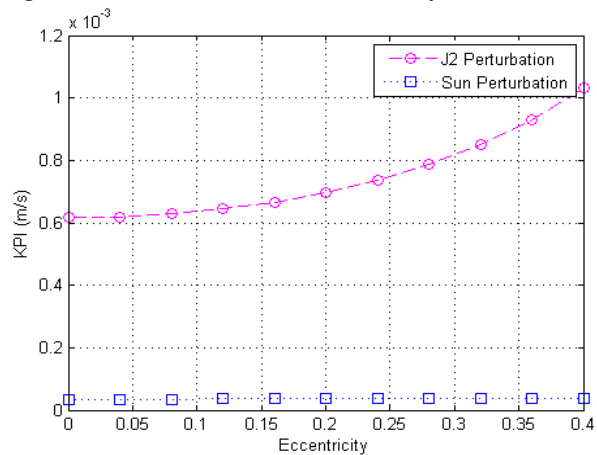Fig. 6: The KPI values as the eccentricity increases.

Fig. 7: The KPI values as the eccentricity increases.

It is possible to note from Figure 6 that, as the eccentricity of the orbit increases, the third-body perturbation also increases. It occurs because, as the eccentricity increases, the distance from the spacecraft to the third-body decreases (at the apogee for Beta and at the perigee for Gama) since the third-body perturbation is proportional to the square of the distance (see Equation 4).

The solar radiation pressure barely changes as the eccentricity of the orbit changes, but there is a slightly decrease. As the eccentricity increase, the distance from the spacecraft to the main body decreases and, therefore, there spacecraft passes through the shadow region in some paths.

Figure 7 shows the effects of the Sun and the J_2 perturbation. The order of magnitude of the effects of the Sun is 3.5×10^{-5} m/s. The effects of the J_2 perturbation vary from 6×10^{-4} to 1×10^{-3} m/s. The order of the magnitude of the J_2 perturbation is also small, if compared to the other perturbations, but it is possible to note that the J_2 perturbation increases exponentially as the eccentricity of the orbit increases. As the eccentricity of the orbit increases, the perigee of the

orbit decreases and, therefore, the J_2 perturbation becomes more prominent as the distance from the main body and spacecraft decreases (see Equation 5).

Figures 8 and 9 are related to the KPI value as the inclination of the orbit changes. The semi-major axis of the orbit was chosen to be 9.3 km and the eccentricity equal to zero.
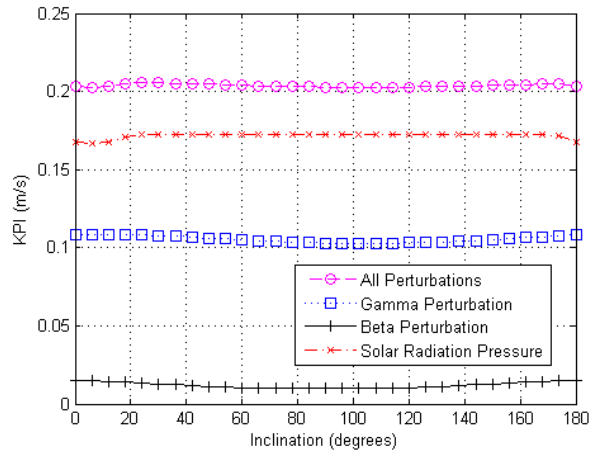

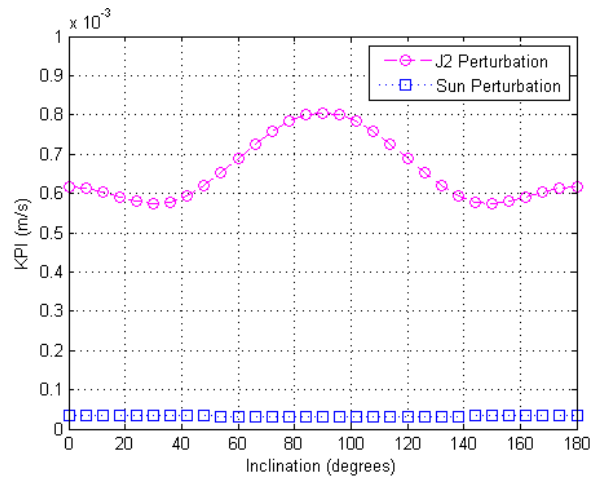Fig. 8: The KPI values as the inclination increases.

Fig. 9: The KPI values as the inclination increases.

In Figure 8, the third-body perturbation has a maximum KPI value when the orbit of the spacecraft and the third-body is the same and a minimum when the inclinations are perpendicular. This occurs because of the geometry of them. When the orbits are coplanar, the distance from the spacecraft's orbit to the third body is smaller if compared to perpendicular orbits (see the first part of the right-hand side of Equation 4).

The solar radiation pressure perturbation has lower values for small inclinations and the minimum value occurs when the inclination of the orbit of the spacecraft is 6.7° (the same inclination for Alpha). The reduction of the solar radiation pressure perturbation for small inclination and the minimum at 6.7° occurs because of

conical projections of the shadow with the positions of Alpha, Sun and spacecraft. Hence, the geometry where the spacecraft has more shadow regions is when the orbits of the spacecraft and Alpha are coplanar.

The minimum value of the KPI considering all the disturbing forces lies at 6.7° of inclination.

Figure 7 shows the perturbation of J_2 and the Sun. It is possible to note that the maximum value of the J_2 perturbation occurs when the orbit has an inclination of 90 degrees and the minimum at 26.57 degrees. The minimum can be found analytically by having the norm of the acceleration in Equation 5 and deriving it by $\emptyset$. The solution has a minimum when $\emptyset = 63.43$ degrees. Regarding that $\emptyset$ is the colatitude of the orbit, then 90-$\emptyset$ is the minimum value at inclination value of I =26.57 degrees. The inclination of maximum value of the perturbation can also be bound by the area of the derived norm of the acceleration versus the co-latitude, which is 90 degrees.

The Solar Sail Usage

The second part of this work aims to use the solar sail in order to reduce the other perturbation forces. As shown in Figures 4 to 9, the most eminent perturbation is the solar radiation pressure. Unfortunately, it is not possible to reduce the solar radiation pressure with the solar sail, once they are originated from the same source and the solar radiation pressure is the most eminent perturbation at the range of the orbits considered. In this way, this second part of the paper will consider the third-body perturbation and the J_2 perturbation as the perturbations that the solar sail aims to control or reduce. The solar radiation pressure will be used now as a control available for the spacecraft, and not a disturbing force. Also, the averaging method will not be used for the solar sail. It will be considered the PI value given by Equation 1 to evaluate the magnitude of the reduction of the disturbing forces.

It was considered two types of solar sail. One can change its area freely, according to the magnitude of the disturbing forces and the second solar sail has a fixed area.

It was considered three initial positions of the Alpha body according to its eccentric anomaly related to the Sun: $E_\alpha = 0$ (perihelion); $E_\alpha = 90°$ (semi-latus rectum); $E_\alpha = 180°$ (aphelion).

The number of orbits considered for the mean value of the PI was 10 orbits of the spacecraft around Alpha. The orbit chosen was: a = 9.3 km, I = 6.7° and e = 0. The initial position of Gamma is $E_\gamma = 0°$ and $E_\beta = 180°$ for Beta.

It was imposed also a maximum area for the variable solar sail area of 80 m^2. The PI values that are not related to the solar sail usage are nearly independent of the position of Alpha with respect to the Sun. They are nearly independent, since the largest disturbing forces

considered in this second part are the third-body perturbation of Gamma and Beta.

The PI value for all perturbations is 0.1089 m/s, where the PI value for Gamma is 0.1083 m/s and 0.0144 m/s for Beta.

The PI values with the solar sail usage vary according to the distance of the Sun. As shown in Equation 6, the solar radiation pressure is proportional to the square distance of the surface with the Sun. In this way, the position of Alpha with respect to the Sun (or its eccentric anomaly) will change significantly the solar radiation energy received by the solar sail panels, since the orbit of Alpha is highly eccentric (e=0.48)[4].

The PI values for all perturbations with the solar sail usage with variable area size are: PI = 0.0639 m/s at the perihelion (see Figures 10 to 13); PI = 0.0682 m/s at the semi-latus rectum; PI = 0.0729 m/s at the aphelion.

As expected, the best reduction of the PI value for the solar sail with variable size occurs at the perihelion (reduction of 41.32% of the perturbation), since at this geometry the solar sail receives more energy from the Sun. At the semi-latus rectum, the reduction is 37.37% of the perturbation and at the aphelion is 33.05% of it.

The results with the solar sail with variable area size show that the solar sail can reduce more than 30% of the perturbations and up to 40%.

Regarding the solar sail with a fixed area of S = 30 m^2, the PI values are: PI = 0.0699 m/s at the perihelion (reduction of 35% of the perturbation); PI = 0.0772 m/s at the semi-latus rectum (reduction of 29%); PI = 0.0850 m/s at the aphelion (reduction of 21.9%).

The reduction of the disturbing of a solar sail with fixed area is slightly worse if compared to a variable area size one. It occurs because a variable size can control the magnitude of the solar sail force and, therefore, reduce more efficiently the disturbing forces.

A solar sail with a variable size can be obtained with the use of a balloon that can inflate and deflate to change its area, so it is not a difficult problem. The choice of which solar sail to use can demand a deep study of the parameters of the spacecraft, the objectives of the mission, the budget, etc.

Figures 10 to 13 illustrates some important results for the solar sail usage with a variable area size at the perihelion of the Alpha's orbit for two spacecraft's orbits.
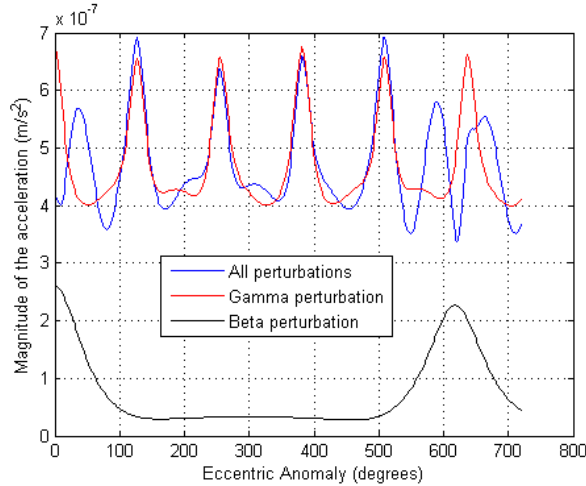
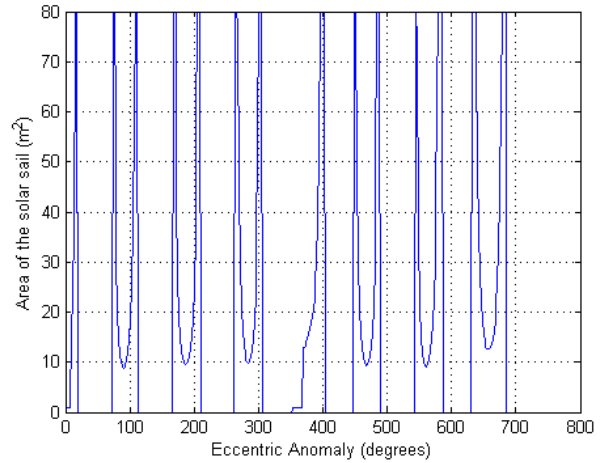Fig. 10: The magnitude of the acceleration of the disturbing forces for two orbital periods.
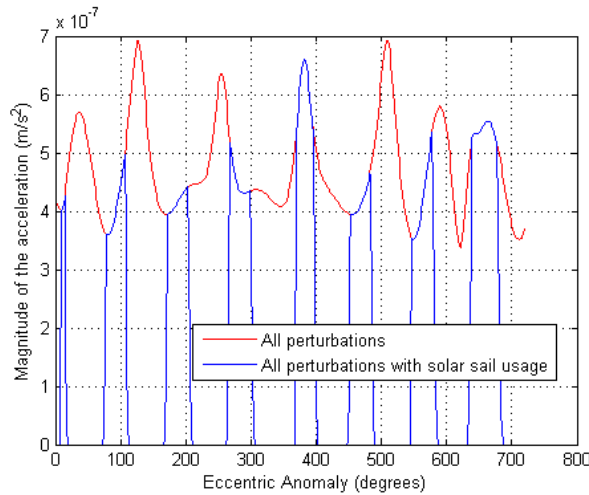

Fig. 11: The magnitude of the acceleration of the disturbing forces for two orbital periods.

Fig. 12: The incidence angle for two orbital periods.

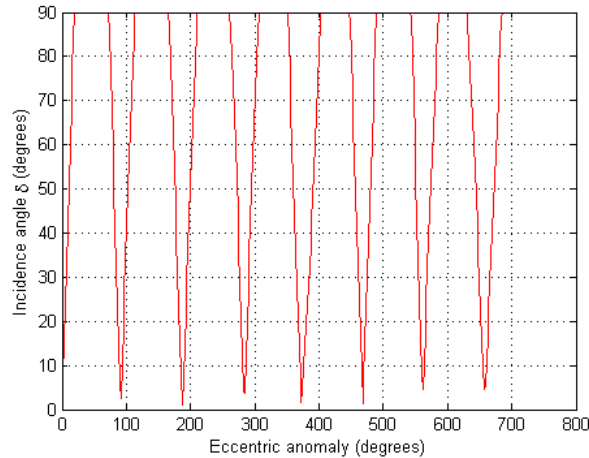Fig. 13: The variable area of the solar sail for two orbital periods.

Figure 10 shows the magnitude of the acceleration for two orbital periods of the disturbing forces of Gamma, Beta and the sum of them. The peaks of the magnitude acceleration of Beta or Gamma are actually when the spacecraft passes through near the bodies. Since Beta is an external orbit compared to the spacecraft, there is less peaks for this perturbation if compared to Gamma (at an inner orbit). The sum of these perturbations is not quite well behaved as the spacecraft orbits Alpha and so do Beta and Gamma, each one with different orbits.

Figure 11 compares the magnitude of the acceleration of the disturbing forces of all perturbations and the magnitude of all perturbations with a spacecraft that uses the proposed solar sail to reduce the other perturbations. It is possible to note that for some intervals, the magnitude of the acceleration of the spacecraft with the solar sail has the same magnitude of the spacecraft without the solar sail. This means that, at the intervals that the magnitudes are the same, the solar sail can reduce completely the other perturbations that act on the spacecraft.

Figure 12 shows the reason why the solar sail can only reduce the disturbing forces for some intervals of the eccentric anomaly. The incidence angle is the key to guarantee that the disturbing force of the solar sail is opposite to the other disturbing forces. Figure 12 shows the optimal incidence angle that guarantees that the solar sail can reduce the others perturbations, but there are some intervals that this incidence angle is larger than 90 degrees. In these cases, the solar sail cannot reduce or eliminate the disturbing forces that act on the spacecraft and it becomes inactive.

Figure 12 shows the area that the solar sail must have in order to guarantee that the magnitude of the acceleration of the disturbing forces is the same. The maximum area imposed for the solar sail was 80 m^2. As

IAC-14-A3,P,42,x24325

shown before, the solar sail with a variable solar sail area can reduce more efficiently the disturbing forces.

IV. CONCLUSION

The integral perturbation method used in this paper was applied in other references before and it has been proved that it can lead to an evaluation of the magnitude of the disturbing forces[9,10,12,12,13,14]. This paper aimed to study the magnitude of the disturbing forces of a spacecraft orbing the asteroid NEA 2001 SN_{263}, since the Brazilian program ASTER aims to send a spacecraft to orbit this asteroid for one year.

The mapping of the disturbing forces based on the perturbation integrals with the help of the averaging technique lead to the magnitude of each disturbing forces that act on the spacecraft for different orbital parameters. The results show minimum values of the magnitude of the disturbing forces, which they point to good orbital parameters to place the spacecraft in order to reduce the shifts caused by the disturbing forces.

The maps can also be useful to evaluate the magnitude of the disturbing forces in case the spacecraft deviates from its nominal orbit and the potential cost of the station-keeping maneuvers.

The usage of the solar sail proposed lead to an interesting result as it can reduce up to 40% of the disturbing forces of the third-body perturbation and J_2 perturbation at the best scenario. The usage of the solar sail can reduce also the shifts caused by the disturbing forces acting on the spacecraft and, therefore, the consumption used to perform a station-keeping maneuver can be reduced.

Whether the mission will use the solar sail or not, the magnitude of the disturbing forces and the maps created by this approach can estimate for an initial analysis of the mission the cost, lifetime and potential orbits that are more feasible for the ASTER mission.

[1] http://www.iau.org/news/pressreleases/detail/iau0602/

[2] http://www.iau.org/public/themes/neo/nea/

[3] Sukhanov A. A., Velho H. F. C., Macau E. E., Winter O. C., 2010, Cosmic Res., 48, 4433

[4] Araujo R. A. N., Winter O. C., Prado A. F. B. A. and Sukhanov A. A., "Stability regions around the components of the triple system 2001 SN263", Mon. Not. R. Astron. Soc. 423, 3058–3073 (2012), doi:10.1111/j.1365-2966.2012.21101.x

[5] Prado A. F. B. A., "Mapping Orbits Around the Asteroid 2001 SN263", Advances in Space Research (2014), doi: http://dx.doi.org/10.1016/j.asr.2013.12.034

[6] Nolan M. C., Howell E. S., Becker T., Magri C., Giorgini D., Margot J. L., 2008, in Asteroids, Comets, Meteors, paper no. 8258

[7] Becker T., Howell E. S., Nolan M. C., Magri C., 2009, BAAS, 40, 437

[8] Fan J., Margot J.-L., 2011, AJ, 141, 154

[9] Prado, A.F.B.A., "Searching for Orbits with the Minimum Fuel Consumption for Station-Keeping Maneuvers: Application to Luni-Solar Perturbations." Mathematical Problems in Engineering (Print), Volume 2013(2013), Article ID 415015, 11 pages.

[10] Oliveira T. C., Prado A. F. B. A., Rocco E. M. and Misra A. K., "Searching for orbits that can be controlled by natural forces", 24th AAS/AIAA Space Flight Mechanics Meeting, Santa Fe, New Mexico, January 26-30, 2014, paper 13-864, 20 pages

[11] Oliveira T. C., Prado A. F. B. A., Rocco E. M. Rocco , "Study of the Fuel Consumption for Station-Keeping Maneuvers for GEO spacecrafts based on the Integral of the Perturbing Forces over Time" World Scientific and Engineering Academy and Society, Brasov, Romania, June 1-3, 2013.

[12] Oliveira T. C., Prado A. F. B. A., "Mapping orbits with low station keeping costs for constellations of spacecrafts based on the integral over the time of the perturbing forces", Publication 2014, DOI: 10.1016/j.actaastro.2014.06.035

[13] Oliveira T. C., Prado A. F. B. A., "Mapping orbits with low station keeping costs for constellations of spacecrafts based on the integral over the time of the perturbing forces", Publication 2014, DOI: 10.1016/j.actaastro.2014.06.035

[14] Oliveira T. C., Prado A. F. B. A., " Evaluating Orbits with Potential to Use Solar Sail for Station-keeping Maneuvers", 2nd IAA Conference on Dynamics and Control of Space Systems (DYCOSS), March 24-26, 2014, Rome, Italy

[15] Tewari A., "Atmospheric and space flight dynamics modeling and simulation with Matlab and Simulink", Boston, MA : Birkhauser, 2007. 556 p. ISBN 978-0-817-64373-7

[16] Capó-Lugo P. A., Bainum P. M.,"Orbital mechanics and formation flying: A digital control approach", First published 2011, Woodhead Publishing Limited ,ISBN: 978-0-85709-387-5

[17] Fieseler, P. D., "A method for Solar Sailing in a low Earth Orbit", ActaAstronautica, Vol. 43, No. 9-10, pp. 531-541, 1998.

[18] Longo, C. R. O. and Rickman, S. L., "Method for the Calculation of the Spacecraft Umbra and Penumbra Shadow Terminatior Points", NASA Technical Paper 3547.